PCCP

COMMUNICATION

View Article Online
View Journal | View Issue

Published on 26 October 2015. Downloaded by University of Washington on 25/12/2015 00:06:06.

Cite this: *Phys. Chem. Chem. Phys.*, 2015, **17**, 30248

Received 10th August 2015,
Accepted 23rd October 2015

DOI: 10.1039/c5cp04755b

www.rsc.org/pccp

Programmable diode/resistor-like behavior of nanostructured vanadium pentoxide xerogel thin film

Zhenni Wan,* Robert B. Darling and M. P. Anantram

Electrical properties of a Cr/V_2O_5/Cr structure are investigated and switching of the device due to electrochemical reactions is observed at low bias (<1 V). Depending on the polarity of the first applied bias, the switched device can behave like a diode (forward sweep first) or a resistor (reverse sweep first). The switching is irreversible and persistent, lasting for more than one month. By performing environmental tests, we prove that water molecules in the atmosphere and intercalated in the xerogel film are involved in the electrochemical reactions. It is proposed that an interfacial layer with reduced oxidation state forms at the Cr/V_2O_5 interface, and creates a higher Schottky barrier due to rise of electron affinity. Different interfacial layer thicknesses in forward and reverse first sweeps are responsible for different *I–V* characteristics in subsequent sweeps. The results suggest future applications of these V_2O_5 thin films in low-power read-only memory devices and diode-resistor networks.

Introduction

Vanadium pentoxide has been intensively studied over the past few decades due to its special electrical and chemical properties. Its orthorhombic layered structure offers a large capacity for conducting and intercalating metal ions, especially lithium and sodium ions, for which it can be used as a cathode material in lithium-ion batteries.[1,2] A persistent and reversible electrochromic effect is also observed in V_2O_5 structures, resulting from intercalation and extraction of ions.[3] In particular, Iwanaga performed nano-scale patterning of V_2O_5 thin films by conducting AFM in air without depositing other ionic compounds as a charge source,[4,5] suggesting that electrochemical reactions involving water molecules are possible in a plain V_2O_5 film.

Electron transport properties of crystalline V_2O_5 are commonly characterized by small polaron hopping (SPH). V^{4+} atoms (vanadium atom with a valence of four) created by thermal agitation and crystal defects induce extra electrons in the system, and electronic conduction occurs by means of electron hopping accompanied by a traveling lattice distortion. Therefore, the conductivity of V_2O_5 can be enhanced by several orders of magnitude after ion intercalation, which significantly increases the concentration of V^{4+} states. Switching behavior has also been reported in V_2O_5 xerogel due to the creation of a conductive channel.[6] However, the application of V_2O_5 as a potential memory material employing its electrochemical properties has not yet been exploited so far.

V_2O_5 nanostructures, including nanowires, nanoribbons and nanofibers, have attracted increasing attention recently, and are used in multiple electrical devices such as field emitters,[7,8] field effect transistors,[9] sensors[10–12] and photodetectors.[13] Nanoscale structures usually have higher surface to volume ratios, thus making it easier for electrochemical reactions to occur. One of the easiest ways to construct V_2O_5 nanostructures is through the sol–gel process. Nanoribbons are formed in deionized (DI) water during a melt-quench process. After the gel is dispersed on the substrate and dried, most physically and chemically bonded water molecules evaporate, leaving a thin V_2O_5 xerogel film consisting of entangled nanoribbons.[14] Recent research has shown that such xerogel films with nano-scale roughness and porous surface could significantly enhance the electrochemical reaction capability compared to crystalline V_2O_5.[15,16]

In this work, we investigate the electrical properties of a Cr/V_2O_5–gel/Cr device structure and observe abrupt switching in the current–voltage characteristics within a low bias amplitude of 1 V. Interestingly, the switched electronic behavior of the device is controlled by the direction of the first applied bias: one is diode-like and the other is resistor-like. Such switching is irreversible and persistent, lasting for over one month. The switching mechanism is studied by performing *I–V* measurements within controlled environments and is attributed to electrochemical reactions at the metal/V_2O_5 interfaces involving water molecules. An interfacial layer with reduced oxidation states and thus lower electron affinity appears to be responsible for the diode-like and resistor-like behavior of the device.

Department of Electrical Engineering, University of Washington, Box 352500, Seattle, WA, 98105-2500, USA. E-mail: jennywan@uw.edu

This journal is © the Owner Societies 2015

Published on 26 October 2015. Downloaded by University of Washington on 25/12/2015 00:06:06.

Characterization

1. Film synthesis

The V_2O_5 thin film is synthesized by a sol–gel process. In this method, V_2O_5 powder was melted in a fused quartz crucible in an air atmosphere at a temperature of 800 °C, and held for 15–20 minutes. The melting temperature of V_2O_5 is 670–685 °C. Then the melt was poured into DI water at room temperature and stirred for 1 hour. This process yielded a yellowish color gel, with V_2O_5 nanoribbons which have hydrated surfaces suspended almost homogeneously in water. This gel was applied to different substrates by a dip coating method. After application, the film was slowly dehydrated in open air on a hot plate with a fixed temperature of 40 °C, which resulted in a xerogel film with a gentle overlapping of the ribbons and thus a good alignment of the *c*-axes normal to the plane of the substrate. The film consists of entangled nanoribbons in the SEM images shown in Fig. 1.

2. X-ray diffraction analysis

The crystal structure of the V_2O_5 xerogel film was obtained by Bruker F8 Focus Powder X-ray diffractometer using an X-ray source of Cu Kα radiation with wavelength of 1.54 Å. Three samples were annealed for 30 minutes at different temperatures (150 °C, 300 °C and 400 °C). One control sample without annealing was also tested for comparison (Fig. 2).

One dominant peak which represents the (001) orientation can be identified in the results, showing a crystalline structure with randomly aligned *ab*-planes, but with well-aligned *c*-axes. Note that even in the sample without any annealing, this peak is significant, indicating that the V_2O_5 nanoribbons have a good alignment in *c*-axis. However, compared to bulk V_2O_5 with (001) peak at two theta values equal to 20.8°, our peaks at 6.9°, 7.1°, 7.9° and 12.3° all show smaller two theta values at the (001) peak. This corresponds to a larger interlayer spacing as a result of the water molecules intercalated between the V_2O_5 layers.[14] Note this is consistent with the fact that an increasing trend of two theta values is observed as the annealing temperature increases, which removes more intercalated water molecules. The full-width half-max (FWHM) of the (001) peak also shrinks and other small peaks appear while the annealing temperature increases. This means that the nanoribbons are distinct at first, but slowly meld together with increase in annealing temperature, making the structure a more uniform crystalline thin film.

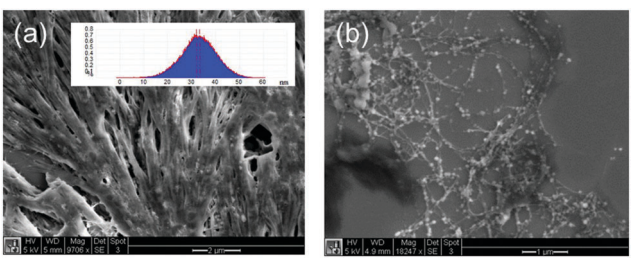


Fig. 1 SEM image of V_2O_5 xerogel film synthesized by sol–gel process. (a) Bulk region of the film. Nanoribbons are entangled and surface is rough. Inset: Surface height profile extracted from AFM data. Surface roughness is around 15 nm. (b) Edge of the film. Single nanoribbon can be clearly observed.

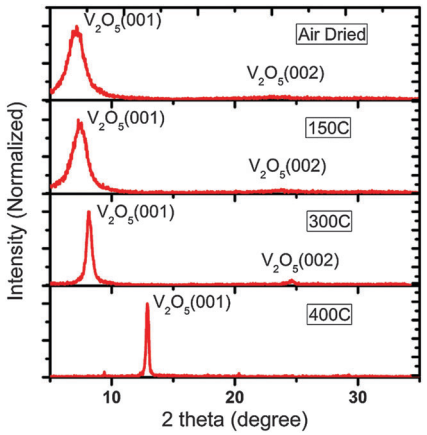


Fig. 2 X-Ray diffraction analysis of V_2O_5 Film. Samples are annealed in air atmosphere at different temperatures for 30 minutes. Air dried and 150 °C annealed samples show similar (001) peaks at around 7° with high FWHM, indicating that nanoribbons maintain their structures with low strength annealing. As the annealing temperature increases, the (001) peak becomes sharper and moves towards higher 2-theta direction, suggesting that the intercalated water molecules evaporate and nanoribbons dissolve due to diffusion, making the xerogel film more like crystalline V_2O_5.

Electrical properties

1. Device structure

A schematic of the tested device structure is shown in Fig. 3. The device consists of a vanadium pentoxide xerogel thin film sandwiched by two metal electrodes. The bottom electrode is fabricated by e-beam metal evaporation. Aluminum with a thickness of 280 nm is deposited on the silicon substrate, and then capped with a thin layer of 20 nm of chromium to prevent oxidation of the aluminum. The V_2O_5 xerogel thin film is then deposited by a dip coating process on top of the bottom electrode. The thickness of the film is uniform and around 900 nm. Surface roughness of the film is characterized by atomic force microscopy and is around 15 nm (inset of Fig. 1). A top

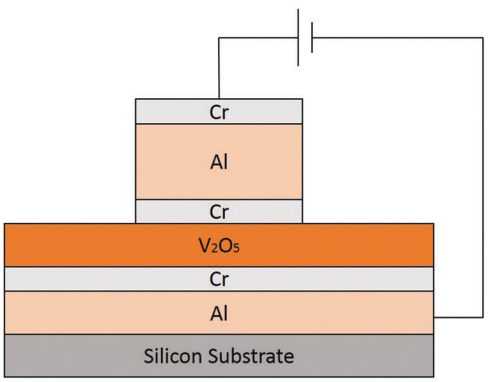


Fig. 3 Schematic of the device structure. The bottom electrode is fabricated on silicon substrate. The V_2O_5 xerogel film is then deposited by sol–gel process. The top electrode is then patterned by shadow mask evaporation.

Published on 26 October 2015. Downloaded by University of Washington on 25/12/2015 00:06:06.

electrode dot with diameter ranging from 1 mm to 10 mm is patterned by a shadow mask during another e-beam metal evaporation. Note that chromium is also used as the interface metal in order to make the device symmetric. 260 nm of aluminum is then deposited to make the top electrode more robust for probe-station measurements as well as to avoid the internal stress of Cr which might crack the electrodes. The aluminum electrode is then capped with another layer of Cr to prevent oxidation. After the device is fabricated, a clean room swab with DI water was used to remove the excess V_2O_5 layer around the top electrode, in order to eliminate the geometrical asymmetry in cross sectional area and offer equivalent gas exposure to both top and bottom interfaces.

2. Current–voltage characteristics in air

The current–voltage characteristics of the device are measured by a custom-built probe station and a Keithley 2612b source meter unit. In the measurements, the bottom electrode is grounded and a voltage bias is applied to the top electrode. Environmental tests are performed inside a custom designed vacuum chamber that can be filled with mixtures of different gases.

Current–voltage measurements of the metal–V_2O_5–metal structure were first performed in air. The device exhibits a low-resistance state under low applied bias (200 mV), as shown in Fig. 4(a). This is characterized as the virgin-state of the device. Electrical switching occurs for the first time when a forward cyclic voltage sweep with magnitude of 1 V is applied to the top electrode. A large hysteresis loop with two distinct peaks (at 0.3 V and 0.7 V respectively) exists in the *I–V* curve (Fig. 4(b)), indicating that the state of the device has been changed. The mechanism for switching is attributed to the change of oxidation states at the top electrode/V_2O_5 interface due to electrochemical reactions. In the subsequent voltage sweeps, the *I–V* curves behave like a diode with clear rectifying features as well as a few peaks (Fig. 4(c)). Note that the magnitude of the dominant peak monotonically decreases in consecutive voltage sweeps, indicating that the reactants, in this case mainly the V_2O_5 at the interface, is being consumed. Further tests under low bias show that the current has been greatly suppressed (>1000 times) with strong hysteresis after the switching (Fig. 4(d)).

We have observed that different scan rates do not change the ability to obtain the transition in resistive to diode like behavior. Fig. 5 shows the *I–V* measurements with different scan rates. With higher scan rates (400 mV s^{-1} and 800 mV s^{-1}), switching is suppressed in the first scan, implying that electrochemical reactions are limited by lack of time. However, repeated scans yield the same behavior as obtained with a single scan with a lower scan rate. That is, switching becomes more pronounced with increasing number of sweeps, further proving the irreversibility of the devices.

Interestingly, the device exhibits an entirely different behavior when a reverse voltage sweep is applied first. Switching with similar hysteresis loop is observed in the first reverse sweep and two peaks show up at −0.3 V and −0.7 V (Fig. 6(b)), implying that the same electrochemical reaction occurs at the bottom electrode/V_2O_5 interface. However, in subsequent sweeps, the device shows a highly linear *I–V* characteristics with little hysteresis; namely a resistor-like state is observed (Fig. 5(b)). Further bias sweeps with a magnitude of 1 V have little influence on the *I–V* curves, indicating that further electrochemical

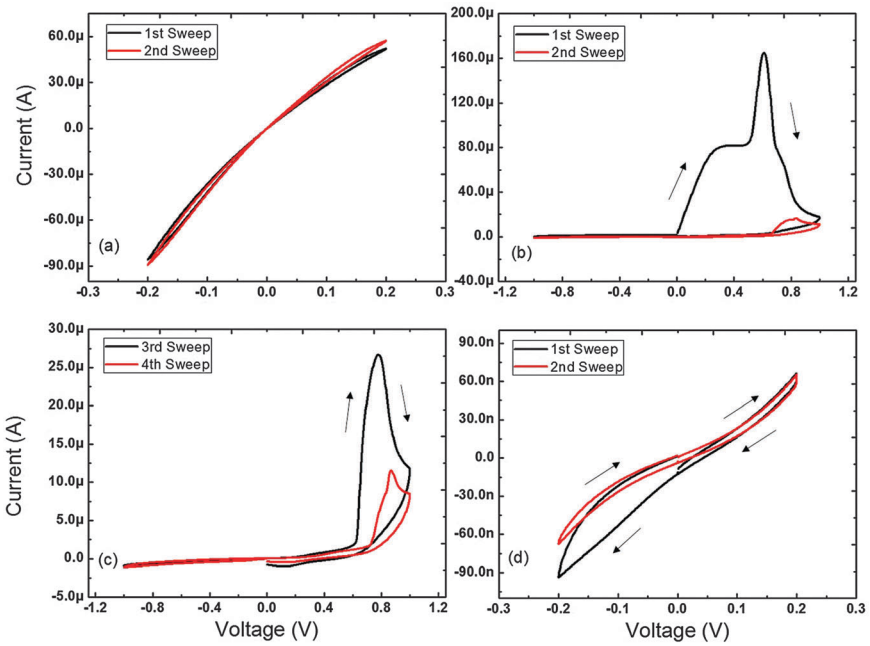


Fig. 4 Current–voltage characteristics of the device in air atmosphere. (a) Low-bias measurements of the virgin-state. The device is in a high conductance state and lasts for over one month if no higher bias is applied. (b) Forward-first sweep. Switching of the device occurs and shows two peaks. (c) Following reverse sweeps. The device remains in a diode-like state with peaks. (d) Low-bias measurements show that device has been switched to the low conductance state.

 This journal is © the Owner Societies 2015

Published on 26 October 2015. Downloaded by University of Washington on 25/12/2015 00:06:06.

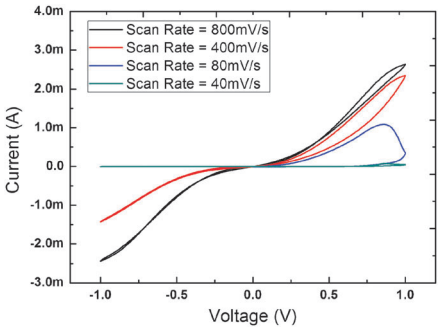


Fig. 5 Sweeps with different scan rates on the same device. 1st sweep has a scan rate of 800 mV s^{-1}, 2nd sweep has a scan rate of 400 mV s^{-1}, 3rd sweep has a scan rate of 80 mV s^{-1}, and 4th sweep has a scan rate of 40 mV s^{-1}.

reactions are suppressed. The low bias current shows that the resistance of the device has increased only by 5–6 times (Fig. 6(a)). Both the diode-like and resistor-like states of the device last for over one month when the device was stored in a vacuum desiccator, suggesting that the switching is irreversible and persistent.

3. Switching mechanism

Vanadium has its highest oxidation state (V^{5+}) in V_2O_5 and has the capability of changing its oxidation state in the presence of reactants and an external electric field. Here, we attribute the reason for the abrupt switching of the device's electronic behavior to reduced oxidation states formed at the Cr/V_2O_5 interfaces, due to electrochemical reactions involving water molecules. To prove our hypothesis and further understand the switching mechanism, *I–V* measurements were performed in a controlled environment.

In Fig. 7(a), the device was measured in a vacuum environment (base pressure $<$ 100 mTorr) for about 5 minutes. It is observed that the switching still occurs during the first forward sweep. In the following sweeps (Fig. 7(b)), the rectifying feature becomes less significant, the hysteresis is reduced and the peak is suppressed, implying that further electrochemical reactions are limited. As a comparison, another device was placed in vacuum for over 2 hours, allowing intercalated water molecules to evaporate. After evaporation, with applied bias, the device shows a diminished switching behavior and remains in a high conductance state after multiple sweeps (Fig. 7(c)), indicating that the intercalated H_2O molecules are responsible for the switching observed in Fig. 7(a). Air was then passed through a drying tube that helps remove moisture, and was used to bring the chamber pressure up to 600 Torr. *I–V* measurements in dry air also show that the switching does not occur (Fig. 7(c)), proving that H_2O in the environment is essential for switching to happen, and the switching of oxidation states is not due simply to the oxidation of chromium electrodes. Finally, a mixture of nitrogen and water vapor is passed into the chamber. In a few minutes, the device is able to be switched again (Fig. 7(d)), indicating that H_2O is sufficient to induce switching. Small bubbles are observed in all the devices after switching, indicating that there are gases released in the reactions. Permanent loss of oxygen is likely to be the reason for the irreversibility of the switching phenomenon.

So far, it is clear that the presence of H_2O molecules is essential for switching the device. With its layered atomic structure, V_2O_5 has the capability of intercalating cations such as lithium and protons. We now provide a detailed hypothesis for the resistance change observed. When a voltage bias is applied to the device, the electric field at the Cr/V_2O_5 interface creates protons from the dissociation of H_2O molecules (eqn (1)). Such a reaction does not occur spontaneously, as the dissociation of H_2O is endothermic and requires external energy.[17] The energy is provided by the electric current, which also explains the long stability of the virgin state. We note that in materials such as TiO_2, the dissociative adsorption of H_2O on the TiO_2 surface is an exothermic process in the presence of oxygen vacancies.[18] The main hypothesis in our explanation is that the dissociation energy of H_2O is reduced when H_2O molecules are intercalated in V_2O_5 layers. The free protons are then driven into V_2O_5 nanoribbons, forming bonds with oxygen (or creating OH^- groups), reducing the oxidation states of V_2O_5 and forming a $H_xV_2O_5$ layer (eqn (2)). At room temperature, the presence of OH^- groups weakens the V–O bonds, making it much easier to remove H_2O molecules and leave oxygen vacancies in V_2O_5 lattice[19] (eqn (4)). At the chromium interface, OH^- groups lose electrons and release

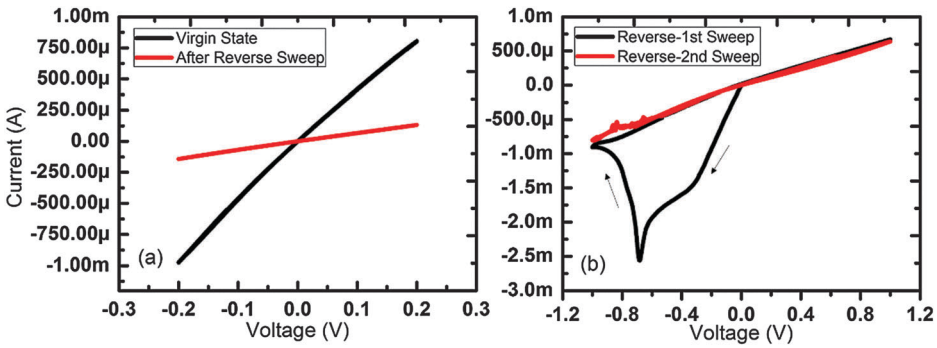


Fig. 6 Reverse-first sweep *I–V* characteristics. (a) Low-bias measurements show that the resistor-like state has only 5–6 times higher resistance than the virgin-state. (b) Switching occurs at reverse bias, and shows similar peaks (−0.3 V, −0.7 V) as forward bias case, but turns the device into a resistor-like state.

Published on 26 October 2015. Downloaded by University of Washington on 25/12/2015 00:06:06.

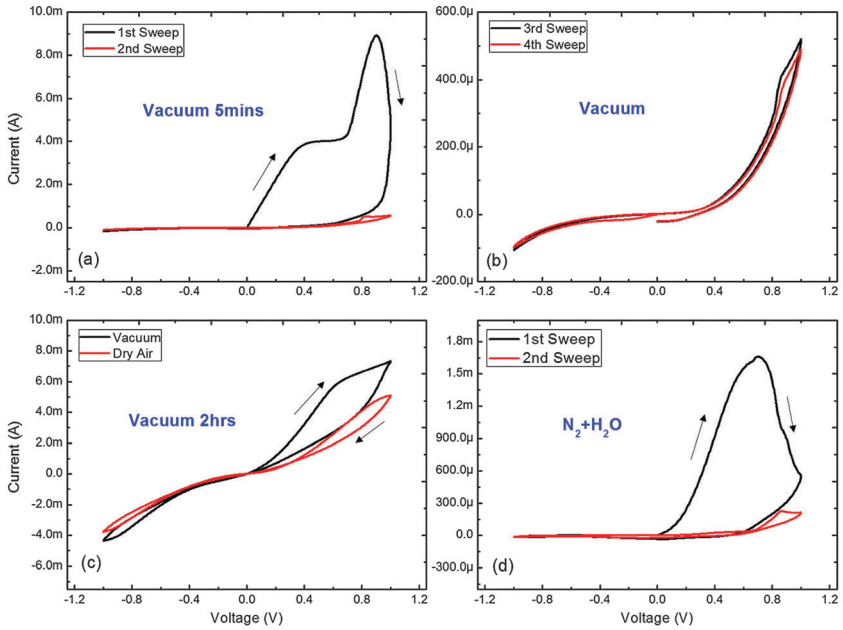


Fig. 7 *I–V* measurements in different environments. (a) Sample is in vacuum for 5 minutes. Switching still occurs as if it were in air. (b) The subsequent sweeps show much less hysteresis and reduced peaks. (c) Sample has been in vacuum for over 2 hours. Switching is highly suppressed due to water removal. (d) The chamber is vented and the same sample in (c) is tested in nitrogen and water vapor. Switching occurs once again.

oxygen gas, creating bubbles in the device (eqn (3)). The complete electrochemical reactions at the Cr/V_2O_5 interface are shown below:

$$H_2O = H^+ + OH^- \quad (1)$$

$$V_2O_5 + xH^+ + xe^- = H_xV_2O_5 \quad (2)$$

$$4OH^- - 4e^- = 2H_2O + O_2 \uparrow \quad (3)$$

$$H_xV_2O_5 = \frac{x}{2}H_2O + V_2O_{5-\frac{x}{2}} \quad (4)$$

4. Asymmetry in two interfaces

The asymmetry in the current–voltage characteristics with two opposite bias polarities indicates that electrochemical reactions only involve interfacial V_2O_5 rather than the whole film, otherwise symmetric electrical characteristics would be observed regardless of the bias polarity. In our hypothesis, electrochemical reactions start from the Cr/V_2O_5 interface to form a V_2O_{5-x} layer, and the thickness of this interfacial layer with reduced oxidation state grows with increasing number of bias sweeps until the applied bias cannot supply enough energy for the electrochemical reactions to occur. The observed asymmetry still stays pronounced after the removal of any excess V_2O_5 layer around the top electrodes, implying that the asymmetry does not simply arise from different exposures to the humidity in the environment, but from the asymmetric synthesis process of the two Cr/V_2O_5 interfaces. Besides, under forward bias bubbles can be observed while there are none under reverse bias, indicating that electrochemical reactions are suppressed in the reverse bias case.

The bottom interface is formed during the sol–gel process of depositing the V_2O_5 xerogel film, in which case the system is exposed to air on a slightly heated (40 °C) hot plate for about 5 hours. A very thin native oxide layer grows on top of the chromium layer during this process, which substantially reduces the reactivity with the subsequently grown V_2O_5 xerogel film. By contrast, the top interface is formed in the e-beam evaporator chamber under high vacuum, where the incident chromium atoms impact the V_2O_5 surface without the presence of any oxygen, thus creating an interface where Cr is fresh without being oxidized. During subsequent bias sweeps, if a reverse bias is applied first, electrochemical reactions occurring at the bottom interface are restricted by the native oxide on chromium as it takes more energy for the electrons bound by OH^- groups to overcome the oxide barrier and transfer to the chromium electrode, resulting in a relatively thin layer of vanadium oxide with reduced oxidation states. In the case of a forward sweep first, the un-oxidized chromium allows the electrochemical reactions to fully take place until all the reactants have been exhausted, implying a thicker interfacial layer with reduced vanadium oxidation states. The asymmetric thicknesses of these interfacial layers with reduced oxidation states are responsible for the asymmetric *I–V* characteristics in the resistor-like and diode-like states of the device.

5. Discussion

In this section, we describe one possible explanation for the underlying mechanism responsible for the diode-like and resistor-like behaviors programmed by the polarity of the first applied bias. Previously it was found that during the voltage sweep, electrochemical reactions occurred at the Cr/V_2O_5 interfaces, introducing a vanadium oxide layer with reduced oxidation states into the system. It has been reported that reduction of

 This journal is © the Owner Societies 2015

Published on 26 October 2015. Downloaded by University of Washington on 25/12/2015 00:06:06.

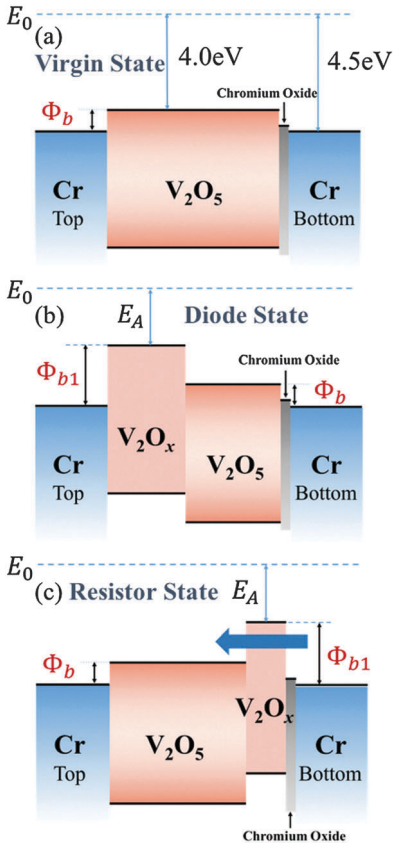


Fig. 8 Band structure of the device. (a) Virgin-state. Chromium has low work function and thus forms a weak Schottky barrier at the interfaces. The device behaves like a resistor in the low bias range. (b) Diode-like state. An interfacial layer with reduced oxidation states forms at the top interface, creating a stronger Schottky contact. (c) Resistor-like state. An interfacial layer is formed at the bottom interface, but with thinner width. Electrons can tunnel through easily.

oxidation states in V_2O_5 will dramatically decrease the electron affinities of vanadium oxide.[20] The band structure of a virgin-state device is shown in Fig. 8(a). The conduction band energy of V_2O_5 is close to the Fermi energy of chromium, forming a low Schottky barrier (Φ_b) for electrons. There is also a very thin layer of chromium oxide on top of the bottom electrode. Note that the electron affinity (E_A) of the chromium oxide is close to the work function of chromium. Thus in the virgin-state of the device, the conductance is high and the contact resistance can be neglected in the low-bias range. When a forward sweep is applied, protons are driven into the V_2O_5 layered structure, and they create oxygen vacancies in the lattice, resulting in a thick interfacial layer with reduced oxidation states (Fig. 8(b)). The electron affinity (E_A) of such an interfacial layer is much lower than the V_2O_5 region, indicating that the conduction band energy rises and thus a Schottky contact with a higher barrier (Φ_{b1}) for electron injection is formed at the top interface. This Schottky barrier is responsible for the diode-like behaviors in the forward-first *I–V* measurements. This increased Schottky barrier is consistent with the polarity of conduction that was observed in the experiments. In the contrasting case of a reverse-first sweep, similar electrochemical reactions will first occur at the bottom interface. However, such reactions are highly limited by the native oxide on the chromium. Therefore, a much thinner interfacial layer is formed in the reverse-first sweep (Fig. 8(c)), resulting a thinner Schottky barrier region through which electrons can easily tunnel. The thin Schottky barrier region increases the contact resistance at the bottom interface to a few times larger than the virgin state. In the following sweeps, the increased contact resistance acts as a voltage divider that limits the voltage drop at both interfaces, thus preventing the occurrence of further electrochemical reactions. Therefore the device remains in resistor-like state.

Conclusion

In this work, we investigate the electrical properties of a metal/V_2O_5 xerogel/metal structure and observe that the device can be switched to diode-like or resistor-like behavior by controlling the direction of the first applied bias. The forward first sweep gives a diode-like current–voltage characteristics, while reverse first sweep results in a resistor-like device. Electrochemical reactions involving water molecules are responsible for the switching, and the switching voltage required is low (<1 V). Both water vapor in the atmosphere and intercalated water molecules in the xerogel film participate in the electrochemical reactions. The switching is irreversible and persistent.

We suggest that an interfacial layer with reduced oxidations states is formed after the electrochemical reactions. Loss of oxygen induces a higher electron affinity in the interfacial layer, and thus a Schottky barrier with higher height is formed at the metal/V_2O_5 interfaces. Such an interfacial layer is thick in the forward first sweep as top chromium electrode is not oxidized so that the energy barrier for electrochemical reactions is low, making the device behave like a Schottky diode. However, the Schottky barrier is much thinner in the case of reverse first sweep, due to limited electrochemical reactions resulting from the native oxide layer on top of the bottom chromium contact. Therefore electrons can tunnel through the barrier easily, resulting in a resistor-like behavior. The results suggest future applications of V_2O_5 to low-power read-only memory devices and diode-resistor networks.

Author contributions

ZW, RBD and MPA came up with the main concepts to realize the device idea presented. The experiments were designed by ZW, RBD and MPA. ZW carried out the experimental measurements. ZW and RBD built the chamber for environmental measurements. All authors contributed to interpreting the results and writing the paper.

Funding sources

UW Startup Grant.

Published on 26 October 2015. Downloaded by University of Washington on 25/12/2015 00:06:06.

Acknowledgements

We acknowledge the use of the Molecular Analysis Facility (MAF) and Microelectronics Laboratory for the chemical and electrical characterization, and the UW NNIN Washington Nanofabrication Facility (WNF) for device fabrication. Useful discussions with Professors Sunil Patil (University of Washington and COEP, India), Stuart Adler (University of Washington) and David Janes (Purdue University) are acknowledged.

References

1 A. E. Semenov, I. N. Borodina and S. H. Garofalini, *In Situ* Deposition and Ultrahigh Vacuum STM/AFM Study of V_2O_5/Li_3PO_4 Interface in a Rechargeable Lithium-Ion Battery, *J. Electrochem. Soc.*, 2001, **148**(11), A1239–A1246.

2 Y. L. Cheah, V. Aravindan and S. Madhavi, Electrochemical Lithium Insertion Behavior of Combustion Synthesized V_2O_5 Cathodes for Lithium-Ion Batteries, *J. Electrochem. Soc.*, 2012, **159**(3), A273–A280.

3 M. R. J. Scherer, L. Li, P. M. S. Cunha, O. A. Scherman and U. Steiner, Enhanced Electrochromism in Gyroid-Structured Vanadium Pentoxide, *Adv. Mater.*, 2012, **24**(9), 1217–1221.

4 R. Darling and S. Iwanaga, Structure, properties, and MEMS and microelectronic applications of vanadium oxides, *Sadhana*, 2009, **34**(4), 531–542.

5 S. Iwanaga, R. B. Darling and D. H. Cobden, Stable and erasable patterning of vanadium pentoxide thin films by atomic force microscope nanolithography, *Appl. Phys. Lett*, 2005, **86**(13), 133113.

6 J. G. Zhang and P. C. Eklund, The switching mechanism in V_2O_5 gel films, *J. Appl. Phys.*, 1988, **64**(2), 729–733.

7 M.-C. Wu and C.-S. Lee, Field emission of vertically aligned V_2O_5 nanowires on an ITO surface prepared with gaseous transport, *J. Solid State Chem.*, 2009, **182**(8), 2285–2289.

8 T. Zhai, H. Liu, H. Li, X. Fang, M. Liao, L. Li, H. Zhou, Y. Koide, Y. Bando and D. Golberg, Centimeter Long V_2O_5 Nanowires: From Synthesis to Field Emission, Electrochemical, Electrical Transport, and Photoconductive Properties, *Adv. Mater.*, 2010, **22**(23), 2547–2552.

9 G. T. Kim, J. Muster, V. Krstic, J. G. Park, Y. W. Park, S. Roth and M. Burghard, Field-effect transistor made of individual V_2O_5 nanofibers, *Appl. Phys. Lett.*, 2000, **76**(14), 1875–1877.

10 N. Vieira, W. Avansi, A. Figueiredo, C. Ribeiro, V. Mastelaro and F. Guimaraes, Ion-sensing properties of 1D vanadium pentoxide nanostructures, *Nanoscale Res. Lett.*, 2012, **7**(1), 310.

11 I. Raible, M. Burghard, U. Schlecht, A. Yasuda and T. Vossmeyer, V_2O_5 nanofibres: novel gas sensors with extremely high sensitivity and selectivity to amines, *Sens. Actuators, B*, 2005, **106**(2), 730–735.

12 H. Y. Yu, B. H. Kang, U. H. Pi, C. W. Park, S.-Y. Choi and G. T. Kim, V_2O_5 nanowire-based nanoelectronic devices for helium detection, *Appl. Phys. Lett.*, 2005, **86**(25), 253102.

13 R.-S. Chen, W.-C. Wang, C.-H. Chan, H.-P. Hsu, L.-C. Tien and Y.-J. Chen, Photoconductivities in monocrystalline layered V_2O_5 nanowires grown by physical vapor deposition, *Nanoscale Res. Lett.*, 2013, **8**(1), 443.

14 V. Petkov, P. N. Trikalitis, E. S. Bozin, S. J. L. Billinge, T. Vogt and M. G. Kanatzidis, Structure of $V_2O_5{\cdot}nH_2O$ Xerogel Solved by the Atomic Pair Distribution Function Technique, *J. Am. Chem. Soc.*, 2002, **124**(34), 10157–10162.

15 S. H. Ng, S. Y. Chew, J. Wang, D. Wexler, Y. Tournayre, K. Konstantinov and H. K. Liu, Synthesis and electrochemical properties of V_2O_5 nanostructures prepared *via* a precipitation process for lithium-ion battery cathodes, *J. Power Sources*, 2007, **174**(2), 1032–1035.

16 D. Vasanth Raj, N. Ponpandian, D. Mangalaraj and C. Viswanathan, Effect of annealing and electrochemical properties of sol–gel dip coated nanocrystalline V_2O_5 thin films, *Mater. Sci. Semicond. Process.*, 2013, **16**(2), 256–262.

17 X. Yin, A. Fahmi, H. Han, A. Endou, S. S. C. Ammal, M. Kubo, K. Teraishi and A. Miyamoto, Adsorption of H_2O on the V_2O_5(010) surface studied by periodic density functional calculations, *J. Phys. Chem. B*, 1999, **103**(16), 3218–3224.

18 R. Schaub, P. Thostrup, N. Lopez, E. Lægsgaard, I. Stensgaard, J. K. Nørskov and F. Besenbacher, Oxygen vacancies as active sites for water dissociation on rutile TiO_2(110), *Phys. Rev. Lett.*, 2001, **87**(26), 266104.

19 K. Hermann, M. Witko and R. Druzinic, Electronic properties, structure and adsorption at vanadium oxide: density functional theory studies, *Faraday Discuss.*, 1999, **114**, 53–66.

20 H.-J. Zhai and L.-S. Wang, Electronic structure and chemical bonding of divanadium-oxide clusters (V_2Oxx = 3–7) from anion photoelectron spectroscopy, *J. Chem. Phys.*, 2002, **117**(17), 7882–7888.

 This journal is © the Owner Societies 2015